PROCESS DEVELOPMENT FOR THREE DIMENSIONAL PRINTING OF METAL LOADED BINDERS

by

MATTHEW PETER GALLA

Submitted to the Department of Materials Science and Engineering on January 14, 1994 in partial fulfillment of the requirements for the Degree of Master of Science in Materials Science and Engineering

Signature of Author_____
Department of Materials Science and Engineering
January 14, 1994

Certified by_____
Professor Michael J. Cima
Thesis Supervisor

Accepted by_____
Carl V. Thompson II
Professor of Electronic Materials
Chairman, Department Commitee on Graduate Students

PROCESS DEVELOPMENT FOR THREE DIMENSIONAL PRINTING OF METAL LOADED BINDERS

by

MATTHEW PETER GALLA

Submitted to the Department of Materials Science and Engineering on January 14, 1994 in partial fulfillment of the requirements for the Degree of Master of Science in Materials Science and Engineering

ABSTRACT

Metal loaded binders were investigated for use in a 3DP process to increase the green density of printed metal parts. Metal slurries and metal loaded waxes were produced and optimized for printing then printability experiments were performed. An extrusion process was developed for printing loaded waxes. A novel process for locking powder with molten polymer was developed and used with the extrusion process for printing three dimensional parts.

Thesis Supervisor: Dr. Michael J. Cima

Title: Norton Associate Professor of Ceramics

Table of Contents

List of Figures and Tables

List of Micrographs

Acknowledgements

I wish to sincerely thank Michael and Eli for all the guidance they have given me. Michael almost always knew "that" formula or reference that unlocked the mystery to the problem at hand and Eli always predicted what would break in my designs. I appreciate the opportunity I have had to work with you both.

I also wish to thank the CPRL crew for being such a good bunch of people, especially Satbir who always bent an ear my way when I needed it.

And to the guys that kept me around and made me feel young, you know who you are.

I want to dedicate this document to my parents, Jay and Leslie, who are the two finest people on earth.

Introduction

Rapid prototyping technologies will potentially reduce development and manufacturing costs for a wide variety of products. These technologies create net shape parts directly from CAD models. Unlike CNC machining, rapid prototyping techniques are based on positive fabrication; material is added to the part in layers, the shape of which are defined by cross sections of the computer model. The layers are created one on top of the other and are bound together *in situ*.

Several rapid prototyping technologies exist, among them: stereo lithography, selective laser sintering, laminated object manufacturing, and three dimensional printing. These technologies can be classified by the method used to define the cross sections that, when bound, create the three dimensional part. Stereo lithography, selective laser sintering, and laminated object manufacturing all use lasers to define cross sections by polymerization, melting, or cutting, respectively. Three dimensional printing (3DP) uses binders that are printed into powderbeds to define cross sections. This distinction allows three dimensional printing to be more versatile in terms of the material that is used to create a part. In particular, 3DP can be used to create metal parts directly from CAD models.

Three dimensional parts are printed by layering thin sheets of powdered material in the Z axis then printing cross sections of the part to be produced into the powder with a binder delivered through an ink jet nozzle (Figure 1). The binder "glues" the powder in the printed region together and subsequent layers are stitched together by matching the binder penetration depth to the

layer thickness. Unbound powder can be removed once the part is finished and the green net shape part is complete. Any powdered material can be used to make the layers and different binder materials can be used to obtain different properties for the completed part.

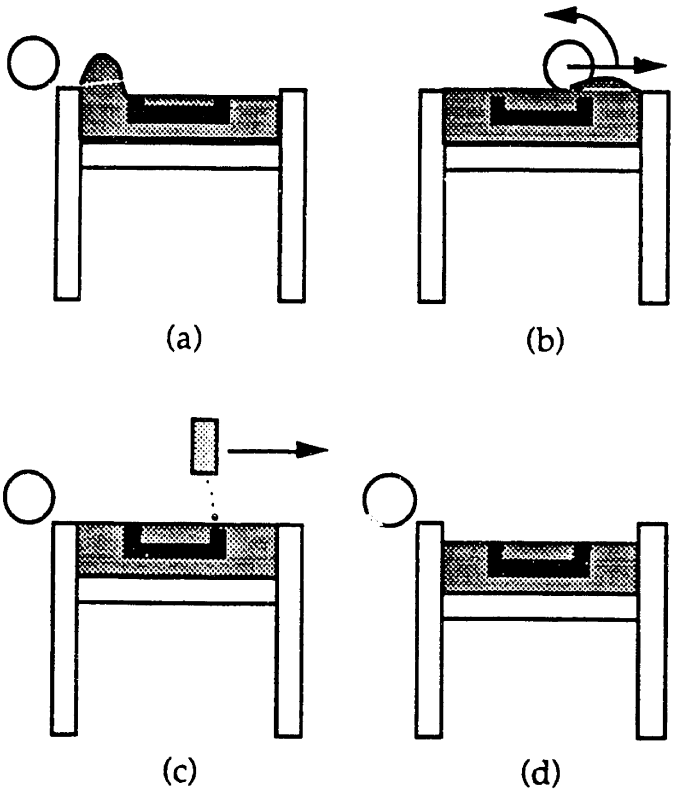

Figure 1. Schematic illustrating the 3DP process. Powder is deposited on a piston (a), powder is spread with a roller (b), binder is printed into the powderbed (c), the piston is lowered (d), and the process is repeated until the part is complete.

Direct printing of metal parts is an important future area for 3DP research. The driving force for this interest is based largely on the possibility of printing tooling for injection molding, die casting, blow molding, and other permanent molding processes. Metal tooling is a major objective for

3DP since the long build times that are characteristic of laminated building technologies can still be faster than conventional tool production methods. Permanent tooling also requires extensive precision machining whereas printed tooling requires little post-machining. In addition, monolithic parts that are printed can contain internal geometries, such as conformal cooling passages, that are impossible to machine.

Production of Metal Parts

Conventional 3DP of metal parts has been used to create complex metal parts and permanent molds. These parts were printed on spherical metal powder with aqueous polymeric dispersions for binding. The packing density of the powderbeds used to build these parts was approximately sixty percent. Thus, forty percent of the original volume had to be either filled or removed during sintering (by shrinkage of the part).

Infiltration of a partially sintered part with a non-ferrous (i.e. lower melting point) alloy is one method used to eliminate void volumes without inducing warpage (Dillon,1984). This method has been used successfully but it compromises hardness and strength of the material which are critical to permanent tooling life and adds cost to the production of a finished part (Ibid).

Increased Green Density Objective

Another route to producing a fully dense part while avoiding warpage is to increase the green density of the printed part. Warpage during sintering is caused by variation of packing density in green parts. Variation in packing density is reduced if material is homogeneously added to the void areas. Figure 2 (a) illustrates the extreme case of a part segregated into two regions of different density. The top half of the part is 60% dense and the bottom is 40% (50% average density). Figure 2 (b) has the same distribution of large particles as (a) but the void volume is filled by smaller particles that are packed to an average density of 50%. The variation in packing density between the two halves of (a) is 60%-40%/2 or +/- 10%. The variation between the two halves of (b) is 80%-70%/2 or +/-5%.

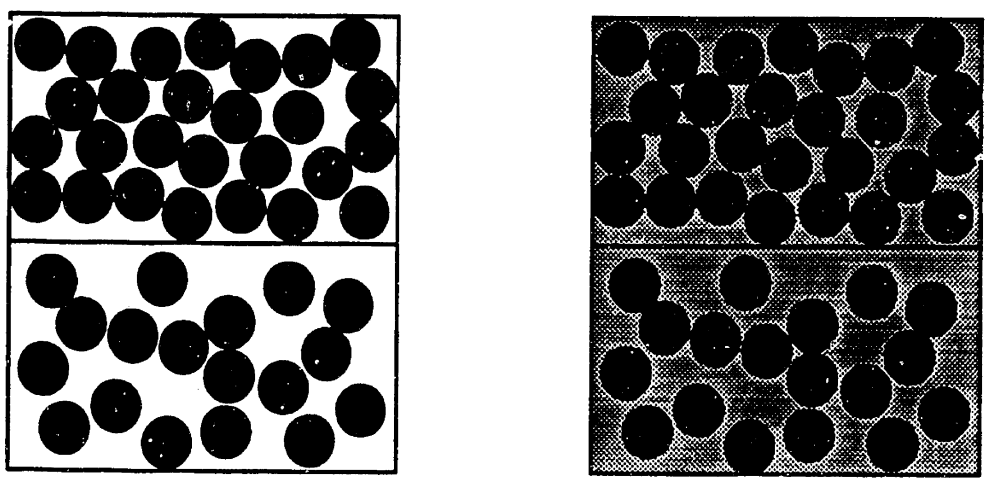

(a) (b)

Figure 2. The variation in packing density in (a) is diminished by homogeneously filling the void space with smaller particles as in (b).

Parts with higher green density sinter to full density with less linear shrinkage (Figure 3). Consider two columns of powder (Figure 4 (a), (b), and (c)) connected by rods. The structure in (a) will look like the structure in (b) after sintering to full density if column 1 has an initial packing density of 60% and column two of 40%. The same structure will look like (c) after sintering to full density if the packing densities of columns 1 and 2 are 80% and 70%, respectively. The combination of higher packing density (less shrinkage) and lower packing density variation (less differential shrinkage) will reduce warpage. Homogeneously increasing the green density of printed metal parts is thus a major focus for 3DP metal processing research.

Methods for Increasing Green Density

Several methods for increasing green density have been proposed, such as bi-modal spreading, tape casting of bi-modal sheets, post-dipping of printed parts, and printing of metal loaded binders. Bi-modal spreading involves spreading a mixture of large powder and a significantly smaller powder wherein the small powder fills a significant fraction of the void space between the large powder particles. Similarly, tape casting of bi-modal mixtures produces sheets of high density that could be cut to the shape of the piston, allowing layers to be stacked instead of spread. Post-dipping of green parts could be carried out in a slurry of small metal powder that infiltrates a part and thus increase density. Finally, metal loaded binders could be printed on existing powderbeds to fill the interstices between powderbed particles thereby increasing the metal density only where the part is printed.

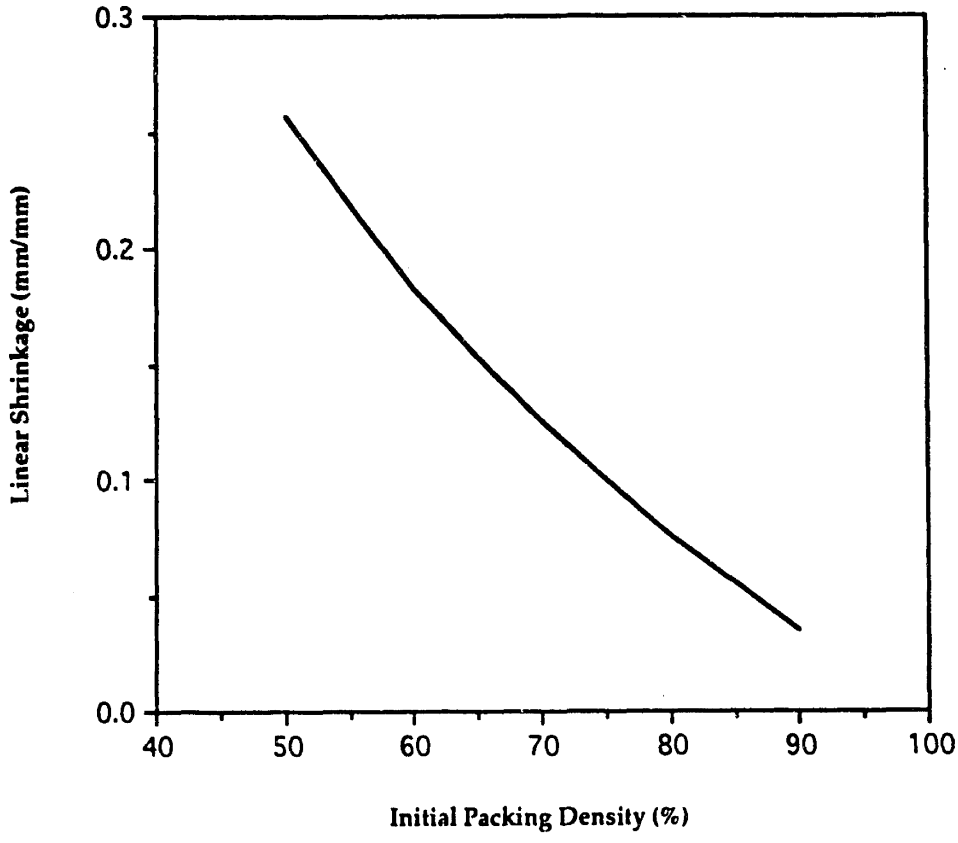

Figure 3. Graph showing linear shrinkage which results from sintering as a function of initial packing density.

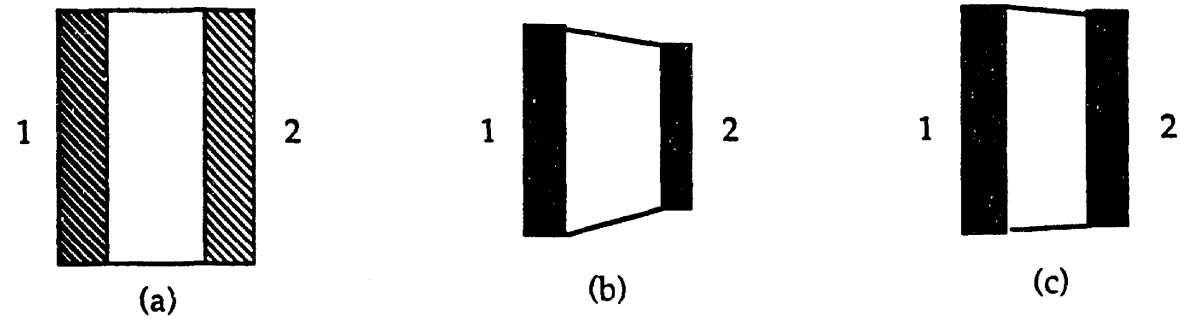

Figure 4. Two columns of different packing density (a), when sintered to full density, will look like (b) when columns one and two have initial densities of 60% and 40% and (c) when 80% and 70%, respectively. [Figure is to scale.]

Previous research on increasing the green density of 3DP metal parts has focused on bi-modal spreading. Attempts to spread bi-modal powders showed major problems with this approach. Segregation of the large and small powders occurs as bi-modal mixtures are spread. Furthermore, bi-modal spreading can only be used to spread relatively large particles.

An alternative method is to selectively increase the metal density only where the part is printed by printing metal loaded binders (Figure 5). This second possibility has three major advantages: 1) homogeneity in the printed part is preserved, 2) material costs are minimized because less secondary material is used, and 3) different secondary materials can be deposited to selectively create microstructures within the same material. Printing of metal loaded binders is the focus of the research reported herein.

Approaches to Metal Deposition

Two distinct methods of metal deposition were considered for research: printing metal slurries and extruding metal loaded wax binders. Slurries, if they can be passed through orifices, are capable of being printed on the existing 3DP machine. Wax binders loaded with metal powder will require an extruder for printing and a heated powderbed to liquefy the binder so it can wick into the powderbed.

A metal loaded binder must be both chemically and physically stable in order to be printed. Chemical stability is mainly a matter of reducing surface

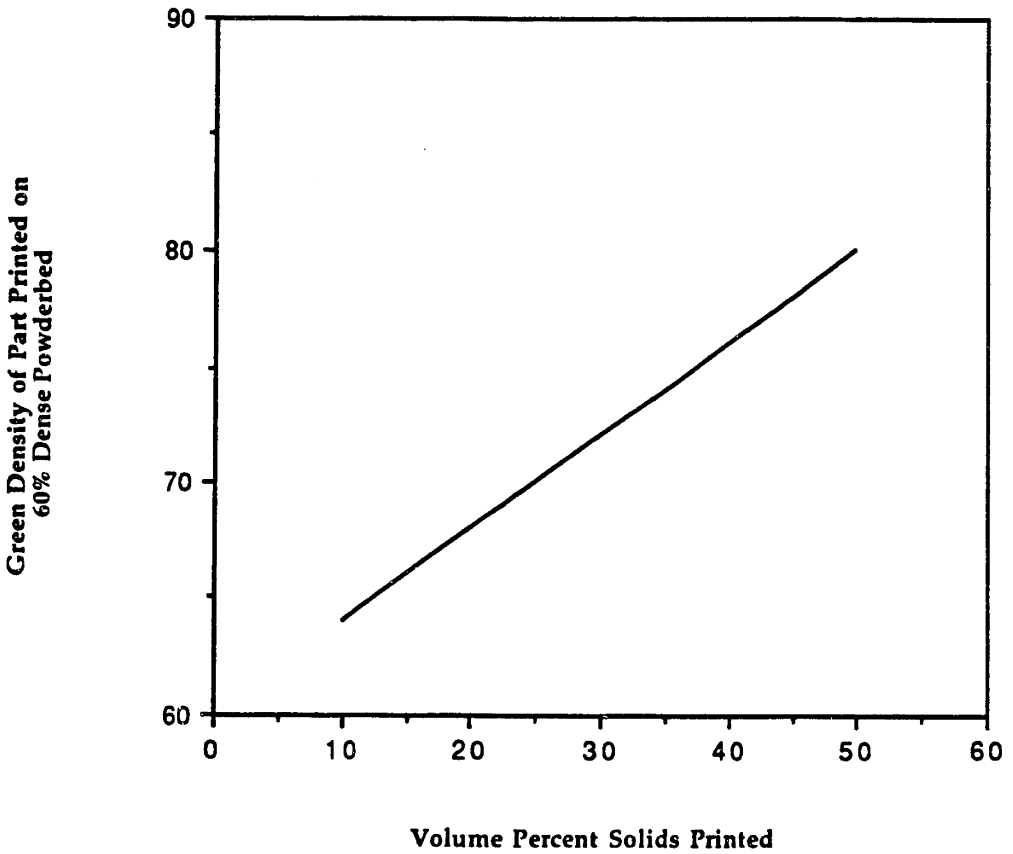

Figure 5. Graph showing increase in green density as a function of volume percent solids printed.

energy within the binder so that no change in state yields a lower energy. Surfactants used successfully to stabilize metal slurries (Adams, 1985) and metal loaded wax binders (German, 1990) have been identified and used in industry. Physical stability is a matter of ensuring that forces acting on the binder from outside sources do not create a lower energy state. The forces that act on the binders are static pressure, gravity, and shear. The static pressure necessary to print these binders is far too low to affect the nature of the

binders, however, the effect of gravity and shear on the binders should be carefully considered.

Stokes' equation for settling particles can be used to estimate the effect of gravity on particles in a suspension. The velocity of a particle settling due to gravity:

$$v = \frac{2(\rho_s - \rho_l)a^2 g}{9\eta},$$

where **g** is the acceleration due to gravity, **a** is the particle diameter, ρ_s and ρ_l are the density of the solid and the liquid, respectively, and η is the viscosity of the liquid. Figure 6 shows the settling velocity of stainless steel particles of various sizes in both heptane and mineral oil. The metal particles are effected greatly by gravity, as the graphs show, and this obstacle will need to be overcome in order to print metal slurries. Metal loaded waxes are not greatly effected by gravity because they are liquid only during and after wicking into the powderbed (wicking takes approximately 1-2 seconds). The metal contained in the wax cannot settle once the liquid wax is completely wicked into the powderbed because it is held in place by the surface energy reduction that caused the wicking to occur.

The shear interaction of particles is detrimental to the physical stability of metal slurries when they are passed through fine orifices. Brady and Bossis showed cluster formation of hard spheres when sheared (Figure 7) with a theoretical model. The simulated viscosity calculations obtained from the same model showed strong shear thickening behaviour for a 0.4 volume fraction solid mixture beyond a critical non-dimensional shear rate (Figure 8). Metal loaded waxes do not induce cluster formation and do not thicken when sheared because they are solid when they are forced through orifices.

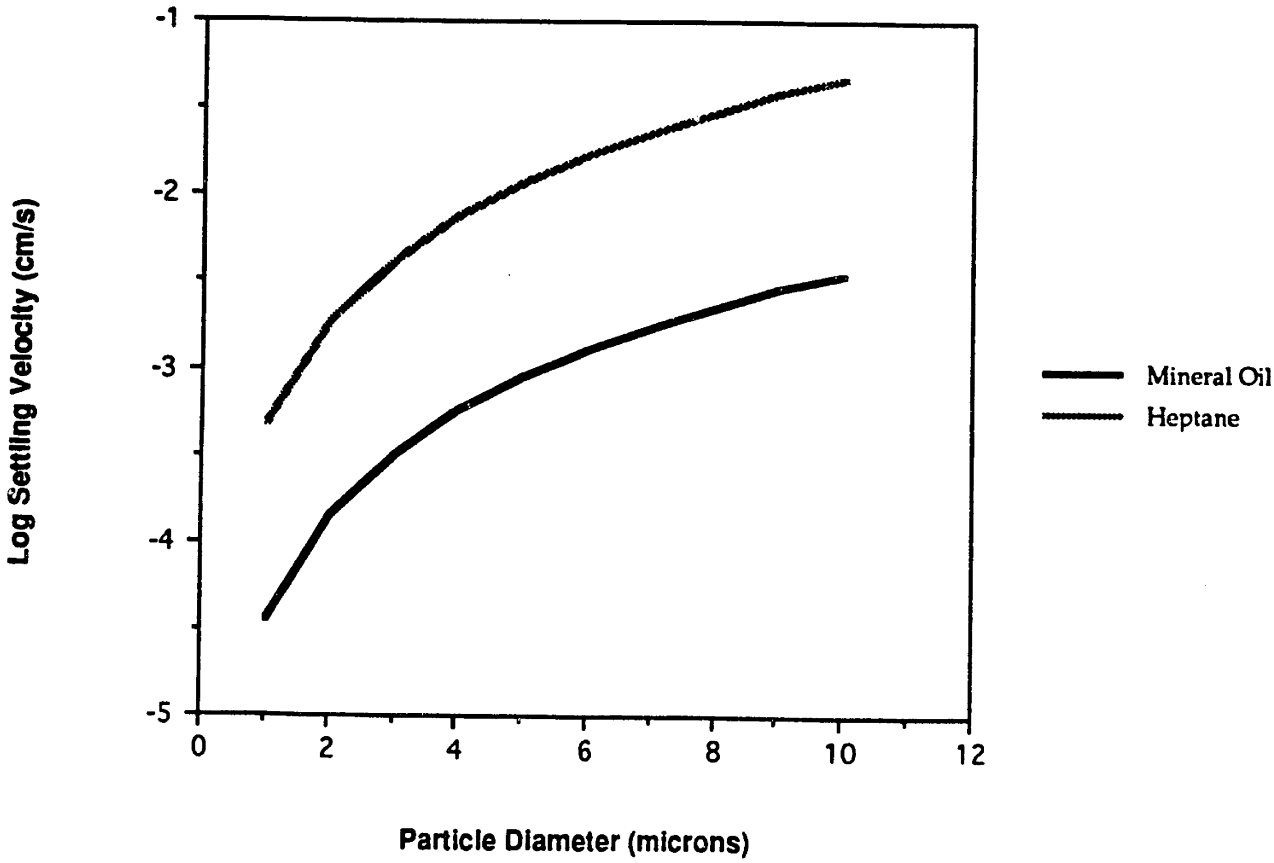

Figure 6. Graph showing the settling velocities of stainless steel particles in both heptane and mineral oil as a function of particle size.

Metal Slurries

It has been shown that chemically stable slurries of metal particles can be produced in non-aqueous fluids (Adams, 1985). Non-aqueous slurries were chosen for investigation of printing in order to preclude problems with metal oxidation through contact with aqueous species. Adams reported stable slurries of copper powder in hexane and heptane with the aid of OLOA 1200 surfactant (Ibid) and his work was the starting point for this research.

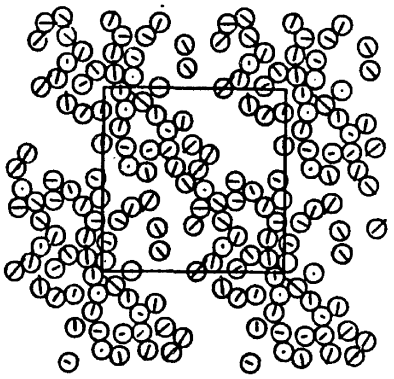

Figure 7. A typical particle configuration of a sheared monolayer of purely hydrodynamically interacting spheres at an areal fraction of 0.4. The bulk motion is to the left at top and to the left at bottom (from Brady and Bossis 1988).

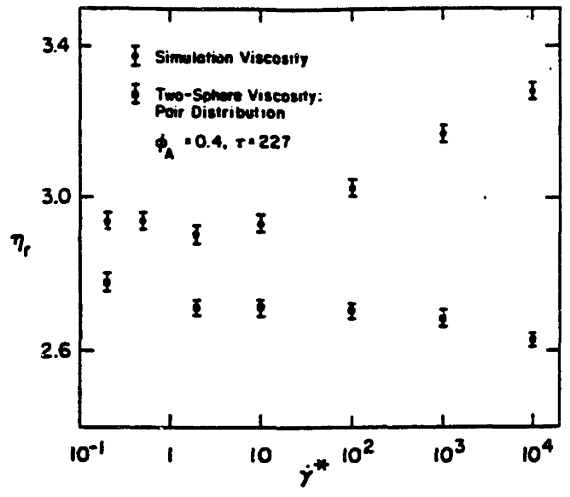

Figure 8. The shear rate dependence of the suspension viscosity for particles interacting through short-range repulsive forces at an areal fraction of 0.4. The simulations show a shear-thickening behaviour due to the increased cluster formation (from Brady and Bossis 1988).

Materials and Equipment

Metal powders used were Cerac 2-3μm copper (C1229), GAF Chemicals 2-3μm carbonyl iron, Johnson Matthey 1.6μm cobalt, and UFT -10μm 316L stainless steel; all powders were spherical and, except for the cobalt, unagglomerated when dry. Other powders were eliminated because of shape and/or degree of agglomeration.

Solvents/oils used were Mallinckrodt laboratory grade hexane, Mallinckrodt laboratory grade heptane, Mallinckrodt laboratory grade toluene, CPRL stock industrial grade mineral oil, and Johnson Matthey laboratory grade light mineral oil (#31911). The liquids were neither purified nor filtered and were used as packaged with only visual inspection as to their clarity.

Two surfactants were used: Chevron Chemical Company OLOA 1200 (determined to be a poly (isobutylene) succinamide (Bishop, 1989)) and Menhaden fish oil. The surfactants were used as provided.

Metal powders and surfactants were weighed on a Mettler PE360 balance and fluids were measured in graduated beakers. Transferring and mixing of powders and surfactants was carried out with stainless steel laboratory utensils. Mixing of the slurries was carried out with either a stainless steel utensil, a electric impeller, or a Waring blender. All slurries were produced in Pyrex glass beakers and settled in either glass beakers or graduated cylinders.

Settling velocities/times were measured either visually with a stopwatch or in a Horiba CAPA-500 particle analyzer. Viscosity experiments were performed on a Haake CV100 rotary viscometer.

Slurry printing experiments were carried out using BD #26 hypodermic needles and syringes, BD #26 hypodermic needles with an in-house produced agitator/pressure chamber, and Stork-Veco .008/.006" orifice plates with an in-house produced, pressurized re-circulation system . Both in-house set-ups were pressurized with nitrogen and powered by a Railpower 2000 toy train transformer.

Slurry Preparation

Several mixing sequences for the materials were investigated in order to obtain suitable slurries: 1) powder was added to mixtures of surfactant and fluid, 2) surfactant was added to mixtures of powder and fluid, and 3) fluid was added to mixtures of powder and surfactant. After several experiments and consultation (Khanuja, 1992), the first sequence was used for the remainder of the experiments.

The solvent/oil and surfactant were measured and combined in Pyrex beakers and stirred until homogeneous. Metal powder was then added slowly to the mixture while stirring continued. Samples mixed with the impeller were also prepared in Pyrex beakers and mixing continued for several minutes after homogenization. Those samples mixed with the blender were prepared in the blender and mixing continued for several minutes after homogenization.

Slurry Experimentation

Several phases of experiments were performed with the slurries : 1) settling experiments testing slurry stability, 2) printing experiments with needle and syringe, 3) printing experiments with needle and agitator, and 4) printing experiments with orifice plates and re-circulation system.

Settling Experiments

Settling times for the slurries were obtained by observing the slurries in glass beakers. A stopwatch was used to record the time in which particles settled three centimeters and settling velocities were calculated from these times. Settling times and velocities for the slurries are recorded in Table 1.

Powder	Particle Size (μm)	Surfactant	Fluid	Settling Time	Settling Velovity (cm/min)
Cerac Copper	2-3	OLOA 1200	Heptane	80 secs.	2.25
		Fish Oil	Toluene	7.3 secs.	24.7
GAF Carbonyl Iron	2-3	OLOA 1200	Heptane	101 secs.	1.78
			Mineral Oil	app. 90 min.	3.3e-2
		Fish Oil	Toluene	8.1 secs.	22.2
UFT St. Steel	10	OLOA 1200	Mineral Oil	8.5 mins.	.352
JM Cobalt	1.6	OLOA 1200	Heptane	4.1 secs.	43.9
			Mineral Oil	43 secs.	4.19

Table 1. Settling time data and calculated experimental settling velocities for metal slurries.

The Horiba particle analyzer was used to obtain more accurate settling velocities for several samples that appeared to settle according to the Stokes' equation. Slurry preparation was carried out next to the Horiba and samples were transferred immediately to the sample chamber in order to get the most accurate results. The Horiba analysis of the copper/hexane/OLOA slurry showed the same particle size distribution as that reported by Cerac for the dry copper powder, thus the settling velocities of the particles were those of a dispersed slurry (Figure 9). Horiba analysis was abandoned because the results did not enhance or refute the results taken from manually recorded settling times.

Printing Experiments

Printability experiments were conducted using needles and syringes. Slurries were drawn into syringes, needles were attached, and slurry was forced through the needles; syringes were shaken constantly to prevent settling. All slurries clogged the needles in less than 10 seconds. Particle settling caused clogging of the needles, but some slurry was forced out indicating that low volume fraction metal slurries are printable.

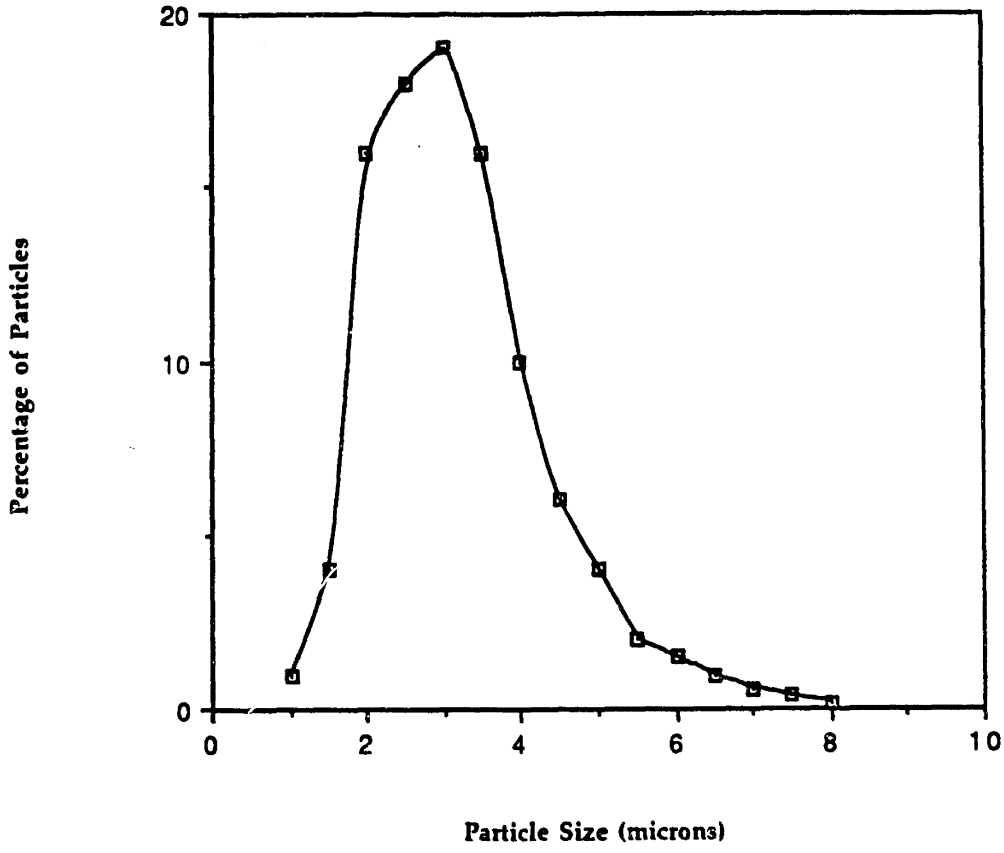

Figure 9. Horiba particle size distribution analysis of Cerac 2-3 μm copper dispersed in heptane/OLOA.

Printability experiments were performed with needles and a pressurized agitator chamber (Figure 10). Slurries were prepared with the impeller then immediately added to the agitator chamber while active. The chamber was sealed and pressurized to force the slurry out of the needle. The agitator was run at full power from the train transformer and the pressure applied was 40 psig. All slurries tested clogged the needles in less than ten seconds.

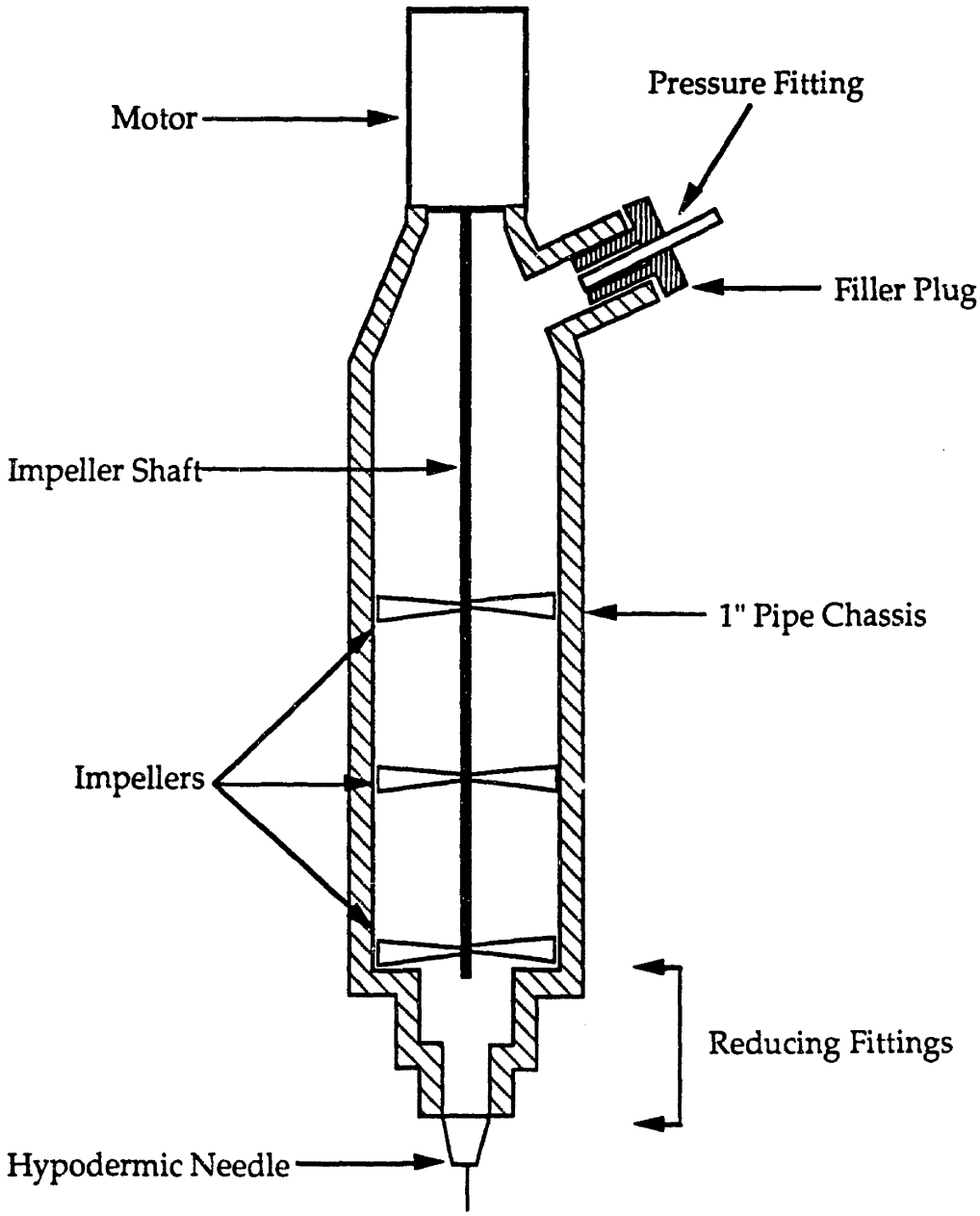

Figure 10. Schematic of agitator chamber used for slurry printing experiments.

Printability experiments were also conducted on the pressurized re-circulation system (Figure 11). Slurries were prepared with the blender, added to the re-circulation reservoir, and the system was sealed. The circulation pump was then activated and pressure was applied. Printing times for slurries tested in the re-circulation system are recorded in Table 2.

Slurry Type	Orifice Size	Volume % Solids	Volume Printed
GAF Carbonyl Iron (2-3 μm) Mineral Oil/ OLOA	150 μm	5	200 ml
		6	200 ml
		7	200 ml
		8	< 5 ml
		10	< 5 ml
UFT Stainless Steel (-10 μm) Mineral Oil/ OLOA	200 μm	5	300 ml
		6	250 ml
		7	250 ml
		10	250 ml
		12.5	< 10 ml

Table 2. Printed volumes of slurries containing diffferent volume percent solids.

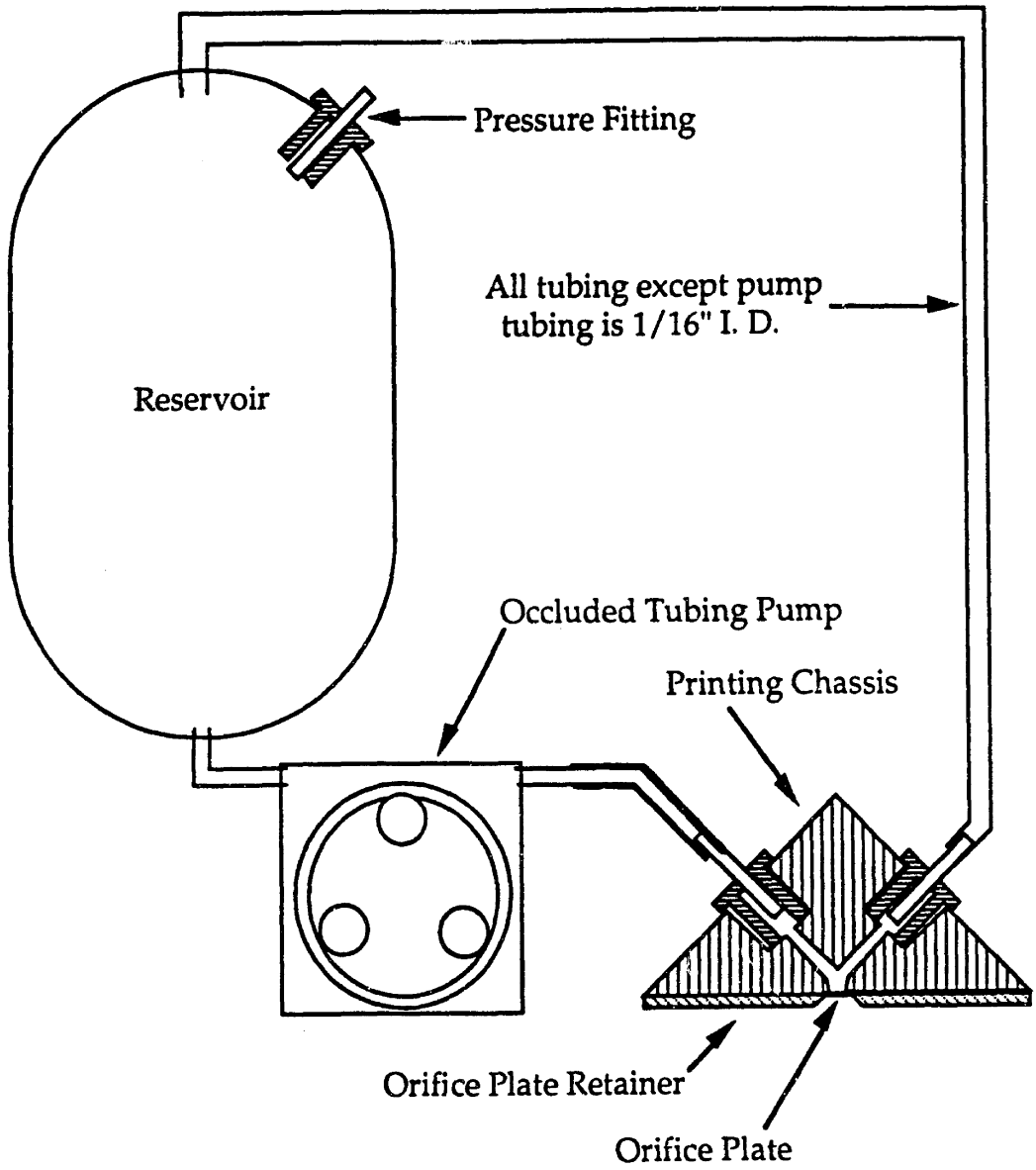

Figure 11. Schematic of recirculating system and orifice plate printhead used for printing experiments.

Settling Results and Discussion

Dispersed metal slurries are more affected by gravity than by Brownian motion of the fluid. Shaw provides the equation for the mean displacement of a particle due to Brownian motion (Shaw, 1970):

$$\bar{x} = \sqrt{\frac{RTt}{3\Pi\eta a N_A}},$$

where R is the gas constant, T is temperature, t is time, η is viscosity, a is particle diameter, and N_A is Avagadro's number. A 10μm stainless steel particle in mineral oil will have a mean Brownian displacement of 9.2×10^{-5} cm in one minute. According to Stokes Law the same particle will settle 0.89 cm in one minute. Thus, viscous drag is the only significant factor suspending the metal powders in the slurries. This is true both because metals have high density and because the size of the particles used in this is on the order of several microns. [Smaller metal powders are available but they are prohibitively expensive and tend to be non-spherical.]

Metal particles dispersed in a fluid will settle according to the Stokes equation whereas aggregates will settle faster. Comparison of experimental settling values to those calculated using Stokes Law indicates that the slurries produced in hexane, heptane, and mineral oil with OLOA 1200 and copper, iron, or stainless steel powders were all dispersed (See Table 3). Cobalt slurries settled faster than the calculated time which can be attributed to the partial agglomeration present in the cobalt powder. An attempt was made to break up the agglomerates by wet ball milling of the slurries, but larger agglomerates resulted due to cold welding. No further cobalt experiments were performed. Comparison of settling data for all other combinations indicates that, as

experimented, no other system produced dispersed metal slurries; these systems were not further examined.

Powder	Particle Size (μm)	Fluid	Fluid Viscosity (centipoise)	Stokes' Velocity (cm/min)	Measured Velocity (cm/min)
Cerac Copper	2-?	Heptane	0.6	1.93	2.25
		Toluene			24.7
GAF Carbonyl Iron	2-3	Heptane	0.6	1.60	1.78
		Mineral Oil	30	3.2e-2	3.3e-2
		Toluene			22.2
UFT St. Steel	10	Mineral Oil	30	.320	.352
JM Cobalt	1.6	Heptane	0.6	.549	43.9
		Mineral Oil	30	1.1e-2	4.19

Table 3. Comparison of velocities calculated from setling times to velocities calculated from Stokes' Equation.

The sample system used in the Horiba (copper, hexane, OLOA) showed exactly what comparison of actual and calculated settling times showed, i.e. the settling particles were dispersed. Only a few Horiba analyses were conducted for two reasons: 1) sample preparation had to be performed at the analyzer (because of rapid settling) and 2) information extracted from the analyses could be more easily and quickly obtained by settling experiments.

Dispersion of metal particles in the systems listed above was achieved by steric separation of particles. OLOA 1200 consists of isobutylene chains that have a bi-functional succinamine group attached to one end (Figure 12) [Bishop, 1989]. The isobutylene chains are soluble in non-polar media but amine groups are not; these amine groups thus adsorb on the metal powder's

surface and the attached chains extend from the particle preventing particle-particle contact.

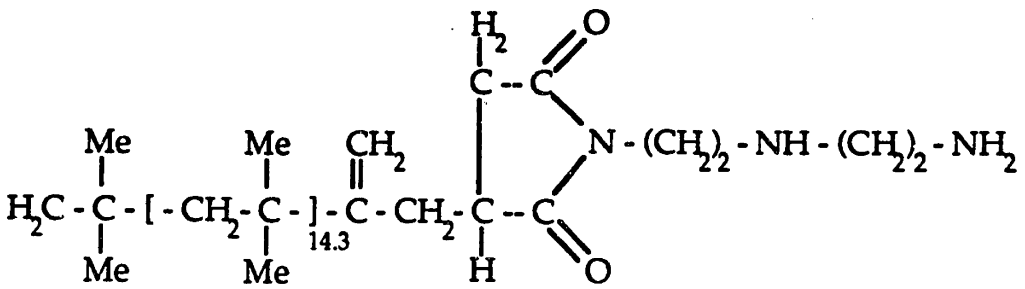

Figure 12. Diagram showing the molecular structure of OLOA 1200. The molecule is a poly (isobutylene) succinamide (Bishop, 1989).

Printing Results and Discussion

The simplest test of printability conceived was to force dispersed slurries through hypodermic needles with a syringe. Clogging occurred in the needles after a short time in each experiment. Settling of the slurries within the syringes resulted in increased slurry concentration at the nozzle which rapidly reached some critical concentration for clogging. This set of experiments showed that the slurries can be forced through small nozzles and confirmed that the obstacle to printability was avoiding high slurry concentration and consequently settling of the metal particles.

An apparatus with a built in agitator was designed and built in an attempt to avoid particle settling (Figure 10). The three impellers inside the chamber were designed to keep the slurry agitated while pressure was applied to the chamber forcing some slurry out of the needle at the bottom of the chamber. If successful, the exiting slurry will have the nominal concentration of the slurry originally added to the chamber. After several experiments it became obvious that the exiting slurry was concentrating even in the small space below the bottom-most impeller (approximately 2 cm) as evidenced by continued clogging.

Three important points had been discovered at this point: 1) metal powders can be readily dispersed in non-aqueous media, 2) such slurries can be passed through nozzles, and 3) rapid settling of metal particles presents the primary obstacle to printability.

Another apparatus was designed to eliminate the problem of settling. The idea behind this apparatus (Figure 11) was to avoid settling by continually circulating slurry through a closed loop of thin tubing. The slurry was forced through an orifice plate that was attached to a small chamber at one point in the closed loop by applying pressure to the entire system. A small volume of slurry was contained in a reservoir and the volumetric flowrate through the entire system ensured that slurry did not dwell long enough in the reservoir to settle. A Masterflex occluded tubing pump was used to circulate slurries through the closed loop because of the abrasive nature of the fluid being pumped through the system. Norprene Food® tubing was chosen to perform experiments because it offered the longest flexure life at the pressures used.

The mineral oil-OLOA 1200 system was chosen to perform the printability experiments because it yielded the lowest settling velocities. The slurry concentration used in these experiments was initially 5 volume percent metal powder and was successively increased until subsequent increase in concentration resulted in clogging. The recirculating volumetric flowrate necessary to avoid settling within the reservoir was determined to be approximately 400 ml/min. and was used for all experiments. The pressure chosen for each experiment was the lowest that produced steady flow through the orifice. This criterion for applied pressure was used because flexure life of the tubing is inversely proportional to the static pressure inside the tubing. The flexible tubing failed consistently between 25 and 30 minutes under 20 psig and between 15 and 20 minutes under 30 psig at the flowrate used.

The problem of settling was overcome as evidenced by the printing times reported in Table 2 (several slurries were printed essentially continually). Up to 200 ml of 7 volume percent iron slurry was passed through a 150 μm orifice and 250 ml of 10 volume percent stainless slurry through a 200 μm orifice each at a flowrate of approximately 10 ml/min. In both cases the limiting factor to volume printed was tubing life. However, printing of low solids volume slurries provides only a small advantage for 3DP of metal parts (see Figures 5 and 3).

Difficulties with Printing Metal Slurries

Reason why higher volume percent metal slurries could not be passed through these orifices were considered. Khanuja (Khanuja, 1994) reports

continuous printing of up to 30 volume percent slurries of 0.7μm (average) alumina in water through 45μm nozzles. Two major differences exist between the success of printing high concentration ceramic slurries and attempts to print high concentration metal slurries: 1) the ratio between nozzle size and particle size for printing of the ceramic slurries was much larger than that for the metal slurry experiments and 2) interaction between particles in ceramic slurries is somewhat different from that in metal slurries.

Brady and Bossis (Brady, 1988) developed a model for simulating shear phenomenon of suspensions that have only short range interparticle forces. Figure 7 (Ibid) shows the formation of clusters when a suspension is subjected to shear. Clusters form despite the repulsive forces that exist between the modeled particles, i.e. the hydrodynamic forces overcome the repulsive forces. Brady and Bossis observed that cluster formation is primarily responsible for viscosity increase and that clusters can transmit stress over "considerable distances". Furthermore, cluster size increases with particle volume fraction and the stress contained in the clusters increases as the cluster size to the third power.

The viscosity increase, or shear thickening, that occurs due to cluster formation is shown in Figure 8 (Ibid) as a function of the dimensionless shear rate. This dimensionless shear rate is

$$\dot{\gamma}^* = \frac{6\pi\eta a^2\dot{\gamma}}{|F_0|},$$

where η is viscosity, a is particle diameter, $\dot{\gamma}$ is actual shear rate, and $|F_0|$ is the force amplitude between particles. The relevant relationship taken from this definition is:

$$\dot{\gamma} \alpha \dot{\gamma}^* x \frac{|F_0|}{a^2\eta}.$$

The actual shear rate required to induce cluster formation and cause shear thickening is thus inversely proportional to the square of the particle diameter and inversely proportional to the fluid viscosity.

The shear rates in the printability experiments performed were calculated to be on the order of 10^5 sec^{-1}. Shear rate is defined as **dv/dl** which is approximately $\Delta v/r$ for an orifice where $\Delta v = v_{center} - v_{wall}$ (assuming a linear velocity profile) and **r** is the orifice radius. The velocity difference is approximately twice the average velocity, which can be calculated from the flowrate. The calculated shear rate is 1.2×10^5 sec^{-1} for a 200 μm orifice and a flowrate of 10 ml/min.

The slurries produced for experimentation contained 10μm particles and mineral oil viscosity is approximately 30 centipoise. Initial viscosity testing of the slurries at low shear rates indicated that shear thickening started to occur at shear rates of approximately 100 sec^{-1} (Figure 13). The Brady and Bossis model indicates that shear thickening begins at the dimensionless shear rate of 10. Correlating the data from the viscometer to the model yields a dimensionless shear rate of 10^4 for the printing experiments. This value can be reduced by using smaller metal powders; reducing the dimensionless shear rate below the critical value for shear thickening requires using metal powders with 0.3 μm average particle size.

It is interesting that the calculated metal particle size appropriate for printing is near that successfully printed for submicron alumina. Khanuja successfully printed 40 vol% slurries of 0.7 μm alumina through a 45 μm orifice. Note also that we routinely print 20 wt% silica sols of nanometer-sized particles. Interparticle repulsion in the ceramic case is electrostatic, while it is

steric for metal powder. Thus, the similarity between the calculated size may only be coincidence.

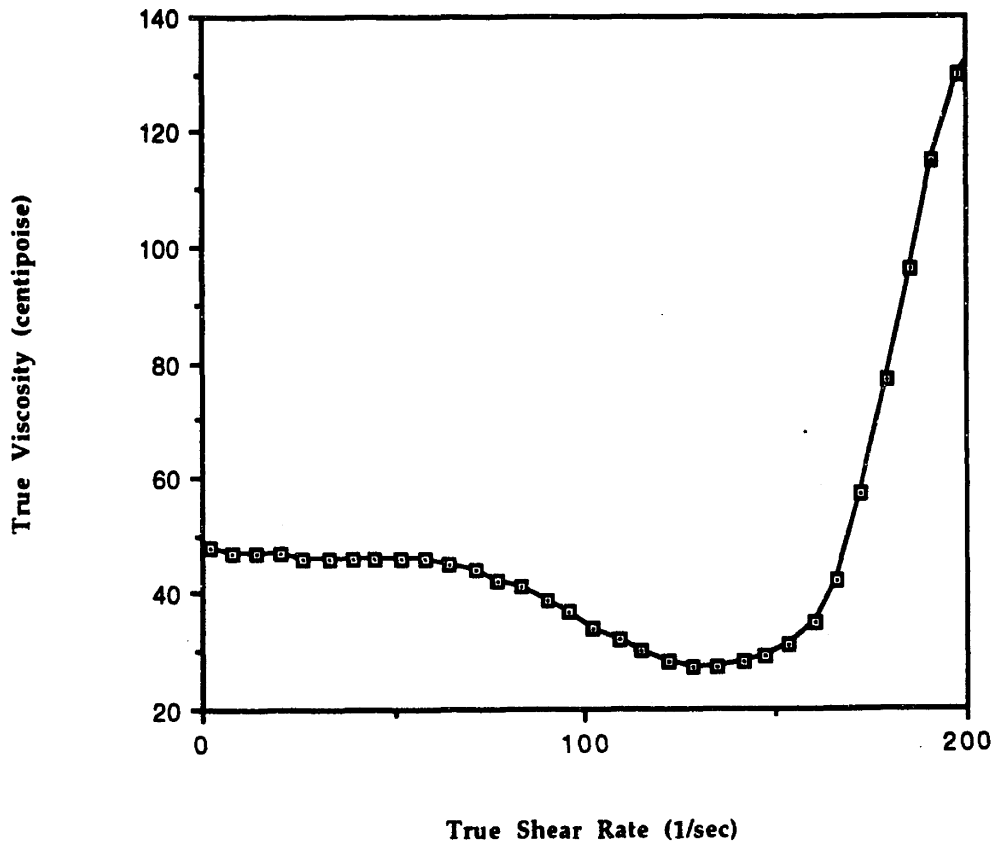

Figure 13. Graph of viscosity versus shear rate data for 10 volume percent, -10 μm stainless steel in mineral oil/OLOA.

Shear induced interaction between metal particles is the main reason why high concentration metal slurries are difficult to pass through nozzles (i.e. without clogging). Several factors contribute to this realization: 1) higher viscosity fluids are necessary to avoid settling, 2) relatively large metal particle

size contributes to easy cluster formation, and 3) shear rates present in the nozzles are high.

Metal Loaded Wax Binders

It was concluded from the above observations that the best binder system for delivering a high volume fraction of metal needs to have a viscosity that can be readily changed by several orders of magnitude. The simplest way to achieve this is to use a low melting point material that can be delivered to the powderbed surface as a solid then melted to flow into the powderbed as a liquid. Two material possibilities were suggested: high molecular weight alcohols and low melting point waxes.

Waxes were chosen for investigation because of their chemical stability, mechanical properties, price, and availability. This choice was based on several simple observations. Waxes are used extensively in molding and other manufacturing operations because of their low melting point, low chemical activity, and ease of forming. Waxes are used as binders for metal injection molding because they have good green strength and can be readily debound to allow complete sintering.

Materials and Equipment

The metal powder used was UFT -5μm stainless steel. This powder was used because it was spherical and readily available. Waxes used were all supplied by Reed Wax and included refined paraffin wax #89040, synthetic wax #89085, and Carnauba wax #1. These specific waxes were chosen based on

their low melting points and low viscosities when melted. These types of wax were chosen because they have been used as binders for metal injection molding (German, 1990).

Two materials that have previously been added to MIM binders were also used: Fisher Scientific stearic acid and Aldrich Chemical low molecular weight polyethylene. Stearic acid has been commonly used in MIM as a wetting agent and die lubricant and polyethylene has been used to increase green strength of parts.

Production of metal loaded binders was performed with the following supplies. Weighing of all materials was done with the Mettler balance listed earlier; heating of waxes and powders was done in Pyrex beakers on a hot stage; combining and mixing of binders was done with stainless steel utensils; homogenization of binders was performed with a heat gun and a Netzsch model 272.01S three-roller grinding mill.

Mechanical delivery of binders for all experiments was performed with in-house designed and built extruders. The extruders were driven by a Canon dc motor and a high torque dc motor, the motors were powered by the Railpower toy train transformer mentioned previously. The extruders were heated by band heaters that were controlled by Omega models CN76000 and CN9000 temperature controllers.

Powderbeds used in printing experiments were all made with UFT -100/+220 mesh 316L stainless steel and some contained the following additives: Fisher Scientific sodium carbonate, Mallinckrodt ferric chloride, Mallinckrodt chromium (II) chloride, and Aldrich Chemical poly (ethylene glycol) with average molecular weight of 3400.

Printing experiments were performed on two Aerotech X-Y mounted translation stages that were controlled by an Aerotech Unidex IV servo controller. The Z-axis for printing (which holds the powderbed) was an in-house designed and built adjustable height piston.

Wax Evaluation

The first objective was to find a wax composition with thermomechanical properties that allowed it to be extruded and with a viscosity, when melted, that is low enough for it to be wicked into a powderbed. All wax mixtures were weighed, combined, and heated in beakers until fully melted then homogenized by stirring. Each wax sample produced was then analyzed qualitatively for thermomechanical and viscous properties.

Thermomechanical Properties

Waxes must soften significantly before melting in order to be easily extruded. The thermomechanical properties of wax samples were evaluated by stirring the waxes with a spatula as they were cooled below their fusion temperature. The qualitative criterion used to classify samples was as follows: samples that deformed plastically below their fusion temperatures were considered for further experimentation whereas samples that cracked or crumbled below their fusion temperatures were deemed unusable for extrusion.

Due to the method of heating (i.e. from the bottom), it was decided to examine the mechanical properties of the waxes produced during cooling from fusion. The pure paraffin wax #89040 was very soft below its melting point, but the synthetic wax #89085 and Carnauba wax #1, both proved to be mostly brittle below their fusion temperatures. Mixtures of the paraffin with varying additions of either the synthetic or the Carnauba wax exhibited softening to a degree inversely proportional to the amount of the addition (as one might expect of a mixture). All mixtures of paraffin with 30 weight percent or less of either of the other waxes met the qualitative criterion imposed.

The temperature at which softening occurred was, however, effected by the amount of the additions. The paraffin melts at 51°C whereas the synthetic wax melts at 86°C and the Carnauba at 96°C; mixtures of the waxes had melting temperatures that were linearly proportional to the percentage of the additions. All mixtures showed softening occur closer and closer to the mixtures melting point as the percentage of synthetic or Carnauba wax increased.

The thermomechanical properties of waxes with additions of low molecular weight polyethylene and stearic acid were also evaluated. Small additions of polyethylene (<5 weight percent) caused crumbling to occur below the fusion temperature in all samples. Additions of stearic acid (up to 20 weight percent) had no apparent effect on the thermomechanical properties of any of the waxes tested.

Wicking Properties

The waxes to be used in printing experiments must readily wick into heated powder. The criterion used to evaluate the wicking properties of the waxes was simple: those waxes that wicked completely into a heated powderbed were acceptable whereas those that did not were deemed unacceptable for use in printing experiments.

A small amount of each wax sample (app. 1 ml) was poured on a heated powderbed (110°C) to test wicking properties. All pure waxes completely wicked into the powderbed as did waxes with stearic acid additions. Waxes with polyethylene additions remained partially on the surface of the powderbed and were thus deemed unusable for printing experiments.

Pure paraffin appeared to be the best base for an extrudable binder because it was desired to use the softest and lowest melting binder for the experiments. Stearic acid has been used as a wetting agent and die lubricant for metal injection molding and proved to have no bad effects on either the thermomechanical or wetting properties of waxes tested. It was decided, for these reasons, to use paraffin plus 10 weight percent stearic acid as the material for producing metal loaded wax binders.

Metal Loaded Wax Binder Production

Metal powder (-5μm stainless steel) was added to molten samples of the chosen binder material to produce metal loaded binders. The metal powder was added both unheated and heated. Cold metal powder added to the molten

wax clumped together and was difficult to separate with stirring. Metal powder heated to 100°C added to the molten wax dispersed readily upon stirring. Preheating of the metal powder was thus chosen as the first step for metal loaded binder production.

Some additional steps were taken to ensure homogeneity of the loaded binders. The first obstacle to homogeneity was settling of the metal powder while the binder was molten. Heated metal additions settled after mixing before the wax binder containing them could cool and re-freeze. This obstacle was overcome by mixing the samples continuously while they were cooled below their fusion temperature.

A step was added to the wax preparation procedure to ensure microscopic homogeneity of the binders. Binders were mixed on a Netzsch three roller mill to ensure that all particles were coated with stearic acid. The binders were milled according to the Netzsch operating instructions except, prior to milling, the rollers were heated to approximately 45°C with a heat gun to help the binder soften. The combined wax/metal samples were slowly added to the mill in small chunks and were mixed. Milling speed and roller spacings were continually tweaked to obtain maximum mixing. During milling, the binders remained soft due to viscous heating. Samples were mixed on the rolling mill for 15-20 minutes after which they were assumed to be homogeneous.

Extrusion of Metal Loaded Waxes

Some of the samples produced by this procedure were then tested in the initial extrusion apparatus (Figure 14). Cooled loaded wax samples were broken into chunks and added to the extrusion cylinder, the cylinder was sealed and heated to 35°C , the head was heated to 50°C, and the ram was activated; the orifice diameter used was approximately 250μm. The extrusion head temperature was lowered while extrusion continued and binder was extruded at temperatures as low as 35°C. The extrusion was not continuous, rather, short sections sporadically shot out because the wax was added in chunks. Small pieces broken off from the O-ring on the piston clogged the orifice and thus prevented extrusion of the entire shot.

An improved extrusion apparatus was designed and built in response to the initial tests with the first apparatus. The new extruder (Figure 15) was designed with only a single band heater and a small extrusion head that screwed directly into the bottom of the extrusion chamber. A single heater was used because the binder was capable of being extruded with only minimal softening and the extrusion head now screwed directly into the extrusion chamber. The extrusion head was designed to be easily removable for cleaning and replacement, and was also designed so replacements (possibly with different orifice sizes) could be easily machined. The O-ring which caused clogging of the orifice was found to be unnecessary, so a simple cylindrical piston was incorporated into the new design.

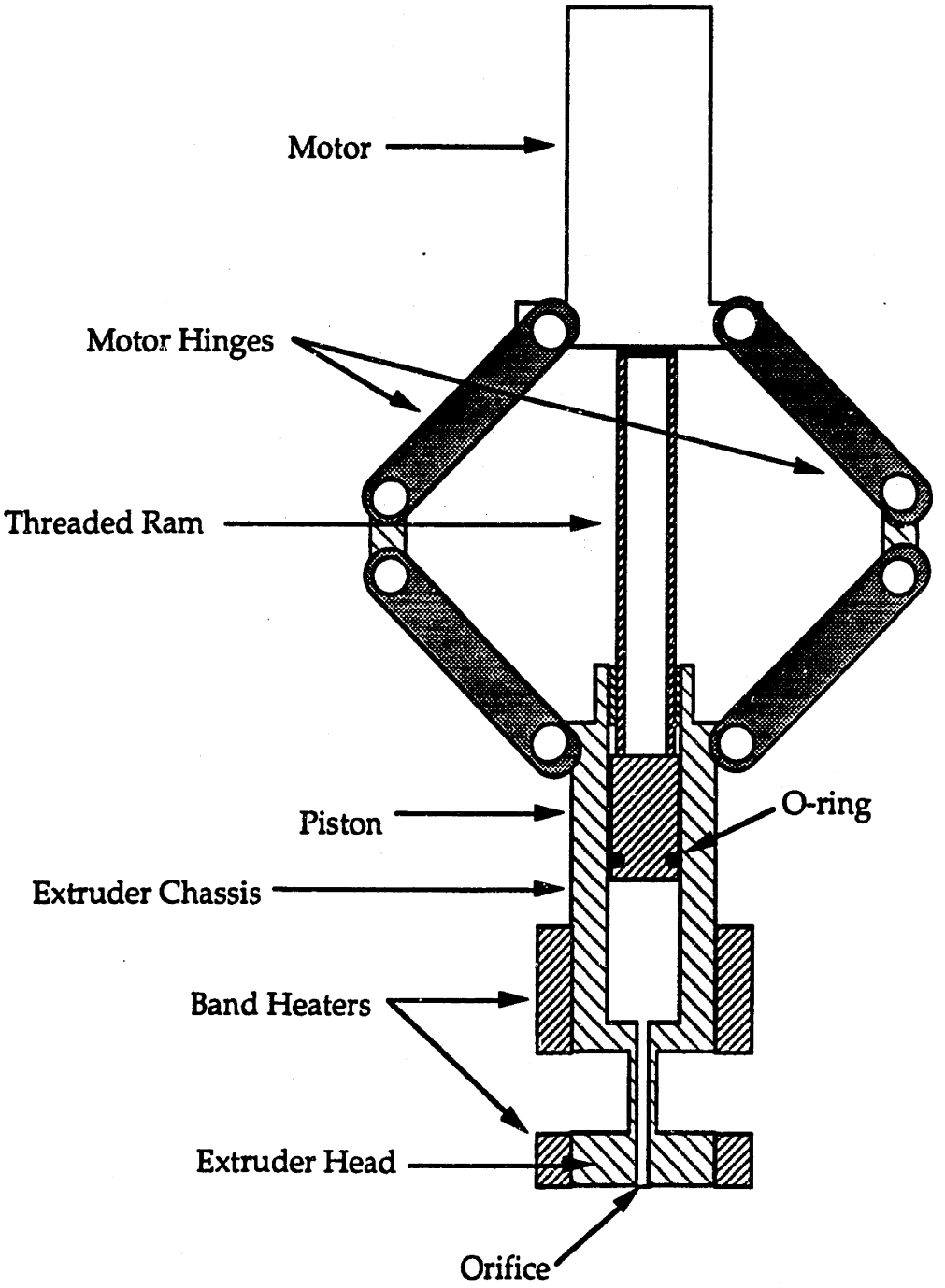

Figure 14. Initial extrusion apparatus with dual band heaters, piston with O-ring, and separate extrusion head.

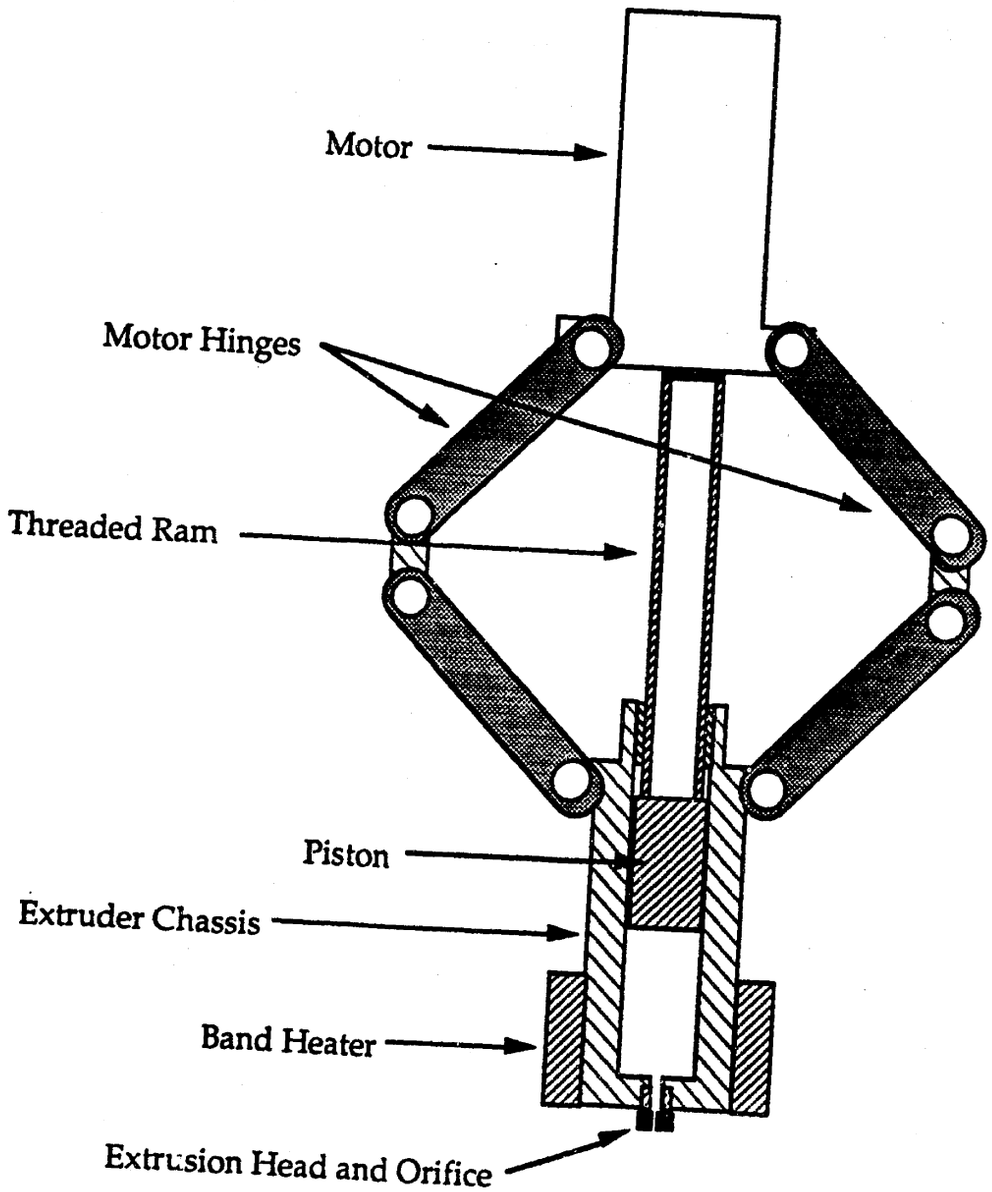

Figure 15. Improved extrusion apparatus with single band heater, piston without O-ring, and integral extrusion head/orifice.

Furthermore, milled binder was melted and cast in a chilled cylindrical aluminum mold in order to from a continuous supply of binder at the extrusion orifice. The mold used had the same diameter as the extrusion chamber. Ingots cast in this mold were used as the extrusion shots in place of chunks of crushed binder.

Cast ingots were extruded in the new extruder into continuous ligaments without clogging. The extruder temperature was varied and chosen to be 37°C based on the ease of extrusion (on the motor) and regularity of the extrudate. The binder was extruded continuously at lower temperatures but the extruder motor was excessively strained; above 38°C the extrudate became less regular due to partial melting of the extrudate at the orifice due to viscous heating. All further extrusion experiments were performed between 36 and 38°C in order to maximize regularity of the extrudate. [The CN9000 controller was always set to 37°C and it maintained the extruder temperature to within +/-1C°.]

Printing of Metal Loaded Waxes

A printing experiment was designed to observe melting and wicking of loaded wax ligaments into a heated powderbed. A block of aluminum with a pocket milled out was attached to a strip heater and mounted to one of the Aerotech translation stages. The pocket was filled with -100/+220 powder that was smoothed with a scraper and the powder was heated to 100°C. The extruder was loaded as before and extrusion was started; after a stable ligament was established, the extrudate speed was matched to the translation speed.

The powderbed was then rastored under the extruder; this process succeeded in placing several ligaments on the powderbed surface.

After cooling, an attempt was made to remove sections of the powderbed (with ligaments still on the surface) to observe why the ligaments did not melt and wick into the powderbed but the result was crumbling of the pieces to be removed. Several crumbled pieces were set with Eastman 910 adhesive, polished, and viewed under the SEM (Micrograph 1).

Micrograph 1 shows that some of the metal loaded binder is present below the powderbed surface, but the majority remained on top. Some powderbed powder is also present on the surface of the ligament which indicates that the wax binder actively wets the powderbed powder.

It is clear from Micrograph 1 that the powderbed was deforming where the ligaments were placed. The SEM sample was difficult to obtain because the printed ligaments had almost no strength. In addition, the samples could not be removed with a section of the powderbed because the large spherical powder is very flowable and thus offers no support.

Printing on Sintered Pucks

Printing on sintered pucks improves our understanding of the process: 1) because they were only lightly sintered, they retained roughly the same pore size and distribution as unsintered powder and 2) the pucks could be used in place of a loose powderbed and samples could be removed with ligaments intact and viewed in an SEM. Micrograph 2 shows a typical region of a sintered puck.

Micrograph 1. Scanning electron image of a cross-section of a line printed on loose powder

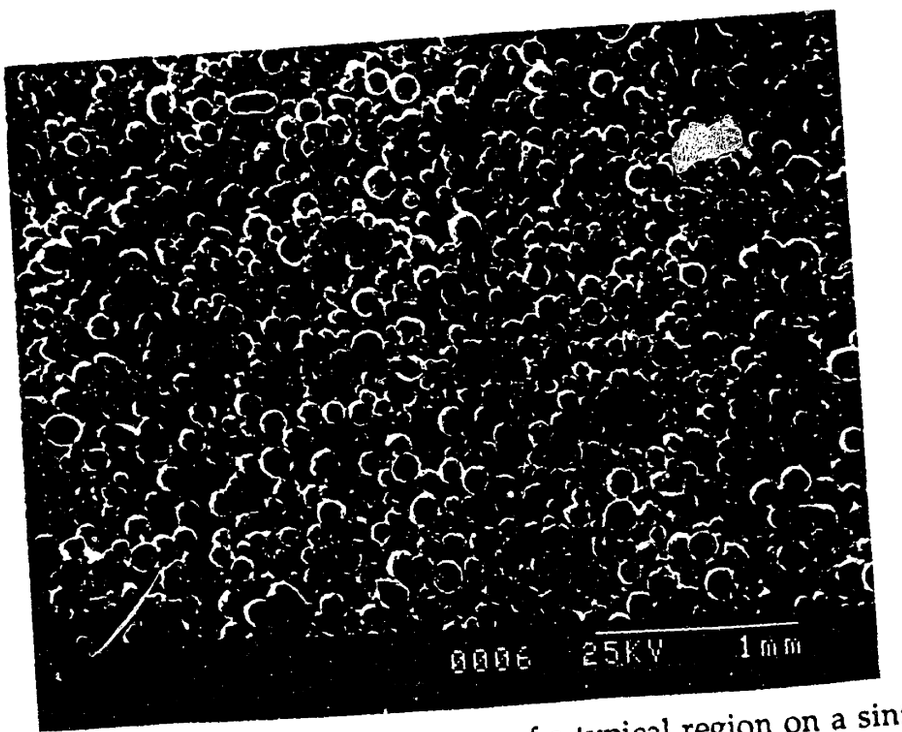

Micrograph 2. Scanning electron image of a typical region on a sintered puck.

Experiments with sintered pucks were performed in an attempt to determine how far the binder (with the same solids loading) wicks into a powderbed. Printing on sintered pucks was very useful for verifying infiltration of the binder but is not suitable for printing 3DP parts because 1) production and layering of sintered sheets is difficult and 2) printed sections could not be removed from the remainder of the sintered powder.

Several flat pucks of lightly sintered -100/+220 powder were produced for printing. Shallow alumina crucibles were filled with powder and heated to 1150°C for 30 minutes. The pucks were removed and, after cooling, the bottom surface of each was determined to be flat.

An experiment was conducted to obtain viewable samples of printed lines. The setup and procedure described above for line printing was used to print lines on the sintered pucks. The ligaments melted and wicked into the sintered puck after printing. This experiment was repeated and the same result was obtained. These samples were heated at 1 C° per minute to 600°C (for binder burnout) then lightly sintered at 1150°C for 30 minutes, sectioned, polished, and viewed in an SEM (Micrographs 3 and 4).

Micrograph 3 shows the cross section of a printed line. The line width and penetration depth are both visible and the surface of the puck (looking into the picture) shows that no printed fines remained on the surface. Micrograph 4 shows a portion of the dense region.

Layer samples were printed on the sintered pucks in order to confirm that the binder consistently wicks into constrained powderbeds. The translation stage used for previous experiments was mounted orthogonally on

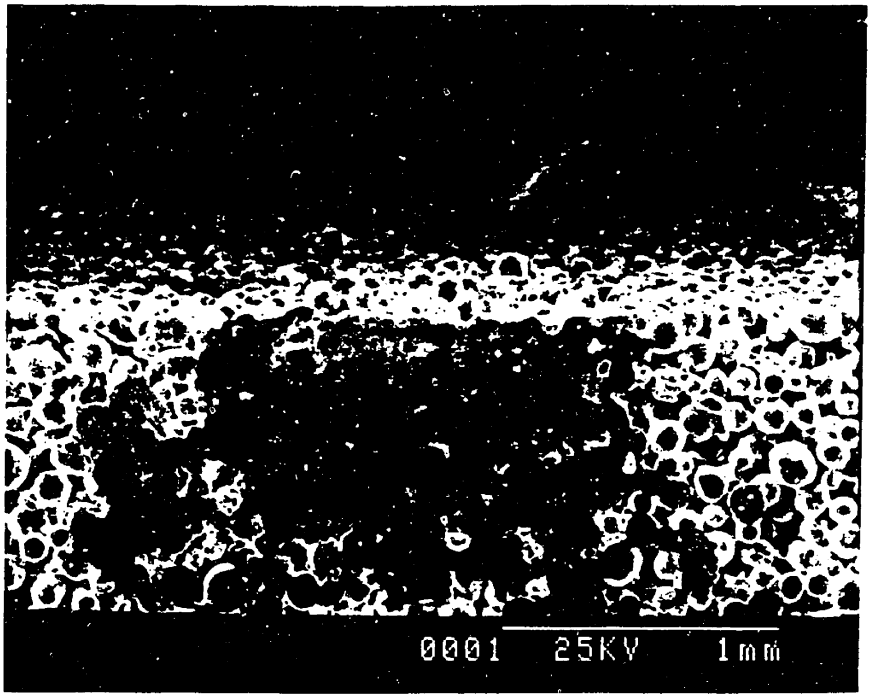

Micrograph 3. Scanning electron image of a cross-section of a line printed on a sintered puck.

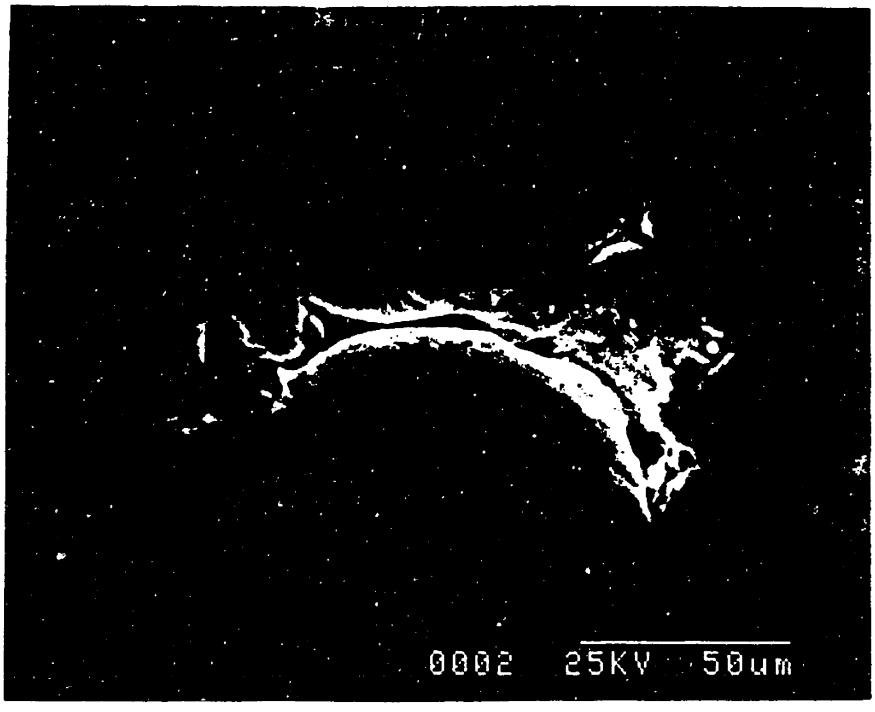

Micrograph 4. Higher magnification scanning electron image of the same cross-section showing dense region.

a similar stage so that X and Y translations could be executed. The X stage that was used for the previous experiments was used with the same parameters and the Y stage was programmed to be indexed one line width between each pass of the X stage.

Examination of single line samples in the SEM showed a line width of approximately 1mm. Printing of the layered samples was done with this line spacing. Two sample sheets were printed with this configuration and complete wicking of the binder into the powder was observed in both sheets. Layer samples were sintered, sectioned, polished and viewed in an SEM as with the line samples (Micrographs 5 and 6). Micrograph 5 shows a cross section of part of the printed layer. Micrograph 6 shows a portion of the dense region.

The line and layer samples printed on the sintered pucks clearly show that the binder wicks into the powderbed if rearrangement of the large particles is prevented.

Powder Locking Experiments

A series of experiments was performed to develop an effective way to prevent movement of particles in powderbed layers after the layers have been spread. Michaels developed a method for "locking" layers in place after spreading in order to reduce ballistic ejection of powder during conventional 3DP of metal parts (Michaels, 1993). This method consisted of mixing powder into an aqueous salt solution, drying this mixture while occasionally stirring (thus dispersing the salt throughout the dried powder), sieving of this powder

to break up clusters, spreading the sieved powder, re-wetting the spread powder with an ultrasonic humidifier, and finally drying the powder in place with a heat gun. This process was reproduced and used as the basis for this set of experiments. Testing of resulting powderbeds was conducted by printing single line samples with a translation stage as done previously.

Three salt solutions ($NaCO_3$, $FeCl_3$, and $CrCl_2$) were prepared: 25 ml each at 40 g/liter concentration and each was combined with 100g of -100/+220 stainless powder. [Sodium carbonate was used because it had been used previously by Michaels and the $FeCl_3$ and $CrCl_2$ were tried because the residual metal is more compatible with the stainless steel chemistry.] These mixtures were placed in porcelain bowls and dried in a Blue M drying oven at 113°C; while drying (approximately two hours) the mixtures were stirred intermittently to prevent caking of the salt. After they were completely dry, the powders were sieved through a #170 brass screen and bottled. The treated powder was spread, subjected to focused ultrasonic mist for approximately one minute (the powder was visibly wet), dried with a heat gun, then single lines were printed on the powders according to established procedure.

When these powders were tested by printing single line samples, only the $NaCO_3$ powderbed had enough strength to prevent rearrangement of the powderbed.

Another means of locking powder in place was proposed. A low melting point polymer can be added to the powder that melts when the powderbed is heated and holds particles together by capillary forces. A solution (25 ml solvent) was prepared with a 40 g/liter concentration of low molecular weight poly (ethylene glycol) and combined with 100g of stainless

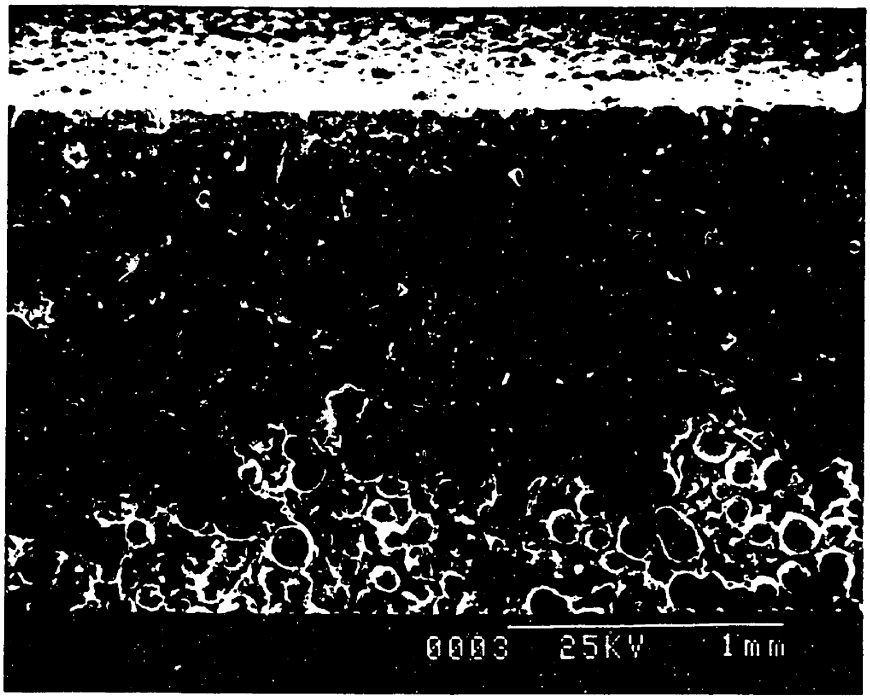

Micrograph 5. Scanning electron image of a cross-section of a layer printed on a sintered puck.

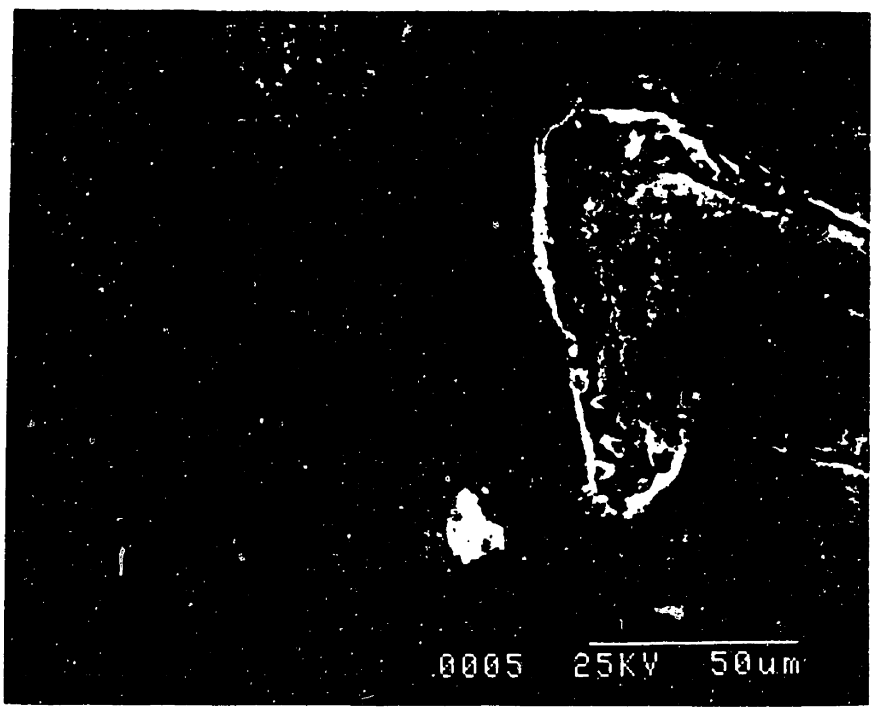

Micrograph 6. Higher magnification scanning electron image of the same cross-sectionshowing dense region.

powder. The mixture/powder was then processed as per Michaels and tested. Testing consisted of spreading the dry sieved powder and then directly executing single line printing procedures. The single line printing tests performed with the PEG showed that this method for locking was also suitable for printing.

The experiments with the low melting point polymer were conducted to simplify the method used for locking. The salt locking method works by re-dissolving the salt that is mixed with the powder then allowing it to dry; the resulting salt bridges form a network of physically constrained powder. This method requires rewetting of the powder between each layer which is time consuming. The polymer method proposed holds powder in place by melting and forming high viscosity liquid bridges that prevent rearrangement by capillary forces. This method has the advantage of not needing rewetting in order to form bridges.

3D Printing on Locked Powder

The sodium carbonate and PEG treated powders were each further tested in a three axis experiment, i.e. successive layers were printed on top of one another. A variable Z-axis (piston) was designed and built (Figure 16) in order to produce layers; the piston utilized screw type height control . The piston top was heated with a band heater and controlled by a CN76000 controller; the piston top height was controlled by turning the height adjustment nut that metered a threaded rod protruding from the piston top.

Three dimensional samples were produced with the $NaCO_3$ and PEG powders using this Z-axis with the X and Y stages used previously to produce layer samples. Some misalignment of subsequent layers occurred due to movement of the piston for spreading of the layers, but partial overlap of the layers yielded several three dimensional structures in the PEG samples; subsequent $NaCO_3$ layers, although overlapped, did not stitch together. A section of the sample from the PEG experiment was separated from the bulk, sintered (as before), sectioned, polished, and viewed under an SEM (Micrographs 7, 8, and 9). The PEG three dimensional structures show that 3DP of metal loaded waxes is feasible but will require much more work before it becomes a reasonable process.

Micrograph 7. Scanning electron image of 3D part printed on PEG treated powder. Note the irregularity of the line spacings yet the continuity between lines.

Micrograph 8. Scanning electron image showing close-up view of one dense region.

This is the most complete text of the thesis available. The following page(s) were not included in the copy of the thesis deposited in the Institute Archives by the author:

p. 55

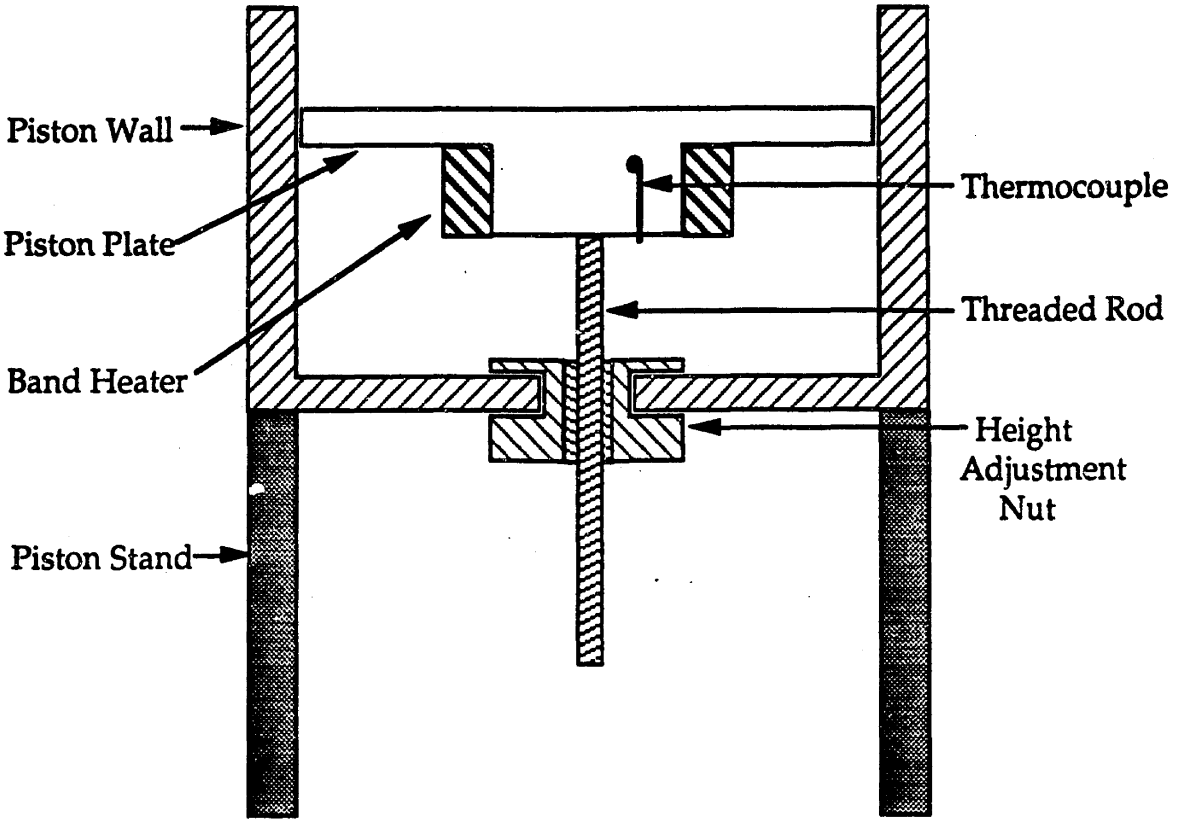

Figure 16. Schematic showing Z axis used for printing three dimensional samples.

Summary of Successful Methods/Procedures

The method for preparation and three dimensional printing of metal loaded wax binders developed in this research is summarized as follows:

Binder Preparation

1) Quantities of paraffin wax (90 weight percent) and stearic acid (10 weight percent) are weighed, combined in a beaker, and homogenized at 100°C;
2) A volume of stainless steel powder (-5μm) equal to 50 volume percent of the total wax binder volume is weighed and then heated to 100°C;
3) After heating, the metal powder is slowly added to the hot binder while the mixture is stirred with a stainless steel utensil (yielding a 33 volume percent metal mixture);
4) This mixture is then cooled below its fusion temperature while stirring continues;
5) The metal loaded binder is then homogenized by mixing on a heated three roller mill for approximately 15 minutes;
6) The homogenized binder is then melted and cast in a chilled aluminum mold into the shape of the extrusion chamber.

Powderbed Material Preparation

1) A 20 gram/liter solution of poly (ethylene glycol) (M_w 3400) in water is prepared by weighing the PEG (1 gram per 100 grams of powderbed powder to be prepared), combining with the appropriate volume of water, and stirring (while heated) until it is homogeneous;

2) The powderbed powder (-100/+220 mesh) is weighed and combined with the appropriate amount of solution in a ceramic bowl that is then heated in a drying oven to 113°C;
3) The mixture is stirred approximately every 15 minutes until the liquid level reaches the powder level, then it should be stirred every 4-5 minutes until it is dry (approximately 1.5 hours total);
4) After drying, the powder mixture is sieved using brass screens to -140 mesh (the agglomerates are broken down by scraping them across the 140 mesh screen) and is then ready for printing.

Printing Sequence

1) The cast solid binder is inserted into the extrusion chamber, followed by the piston, and the drive mechanism is attached to the chamber;
2) The extruder is mounted to the X-Y stages and the height from the powderbed is adjusted to be approximately 3 mm;
3) The Z-axis is lowered approximately 3 mm and powderbed powder is added and leveled manually with a piece of aluminum round stock (this creates a base layer for printing);
4) The powderbed is heated to 100°C and the extruder to 37°C, each is held at these temperatures by the temperature controllers and band heaters;
5) When both controllers have settled at the proper temperatures, the extruder is activated with 10 volts supplied to the motor;
6) The translation stages are then activated by starting a programmed pattern on the Aerotech controller;

7) After the pattern is complete, the extruder is turned off and the powderbed is cooled approximately to room temperature;
8) The Z-axis, and thus the powderbed, is lowered 0.5 mm and a new layer is spread as before;
9) This process is then repeated from step four to obtain the desired number of layers.

Suggestions for Future Work

The initial phase of research on printing metal slurries showed that low volume fraction slurries are printable. The likelihood of employing these slurries in a 3DP process is low. Printing a 10 volume percent slurry into a 60 volume percent powderbed increases the green density of a part by only 4 percent. This gain in green density is not significant enough to warrant further development of the slurry printing process at this time.

However, the slurry printing process does warrant development if sub-micron metal powders become available for a reasonable price. Reducing particle size to 0.3 μm was shown to reduce dimensionless shear rates by three orders of magnitude. Higher volume fraction slurries could thus be printed without clogging. In addition, the settling behaviour of such slurries is much slower than for 10 μm particle slurries. The 0.3 μm particles have a mean Brownian velocity of 5.3×10^{-4} cm/min. and a Stokes' settling velocity of only 8.9×10^{-4} cm/min. Thus, suspended 0.3 μm particles settle microns per minute rather than millimeters per minute.

The extrusion process has shown promise for being a feasible method of producing high green density metal parts. Research on metal loaded wax binders showed that higher volume fraction binders can be extruded and used to print lines, layers, and three dimensional parts. Further development of this process must address several issues before parts can be produced in an actual 3DP process.

The first major issue is binder control. Three parts of the present extrusion apparatus/process are problematic in this sense: 1) the binder leaving the extruder is soft and thus can "wander", 2) the binder continues to extrude briefly after the extruder motor is stopped, and 3) no method currently exists to start and stop binder delivery on demand.

The first two problems are directly related to the softness of the wax. The extruder temperature, which controls softness, was chosen because lower temperatures put excessive strain on the extruder motor (the reduction gears in the Canon motor actually fractured). A more powerful motor must be employed to allow stiffer wax to be extruded. Extruded ligaments must be more like rigid rods than pliable cables. In addition, the wax within the extruder must be stiffer. The extruder is a positive displacement device, but residual pressure inside the extruder causes wax to extrude after the motor is stopped. The wax will not relax if the extruder temperature is sufficiently low.

The third problem is more complex. Printed ligaments must be cut to the proper length to produce lines of a given length. Several methods have been proposed for severing printed ligaments. The first method entails cutting the ligament at the extrusion orifice. The cutting blade, in unison with the motor, cuts the ligament when the motor stops and retracts when the

motor starts. The blade thus serves the dual purpose of cutting the ligament and blocking the extrusion orifice (Figure 17). The second method consists of breaking the ligament inside the extruder by injecting an oil into the extrudate flow (Figure 18). Both of these methods require intricate extrusion head design and the latter requires high precision machining.

The second major issue is feature size. Presently, the feature size is approximately 1mm. The feature size must be smaller for this process to be feasible, thus a smaller extrusion orifice must be used. Orifices for the present experiments were machined with pivot drills and a micro-chuck. Smaller orifices require machining operations which are not available in most machine shops. Furthermore, smaller extrusion orifices require higher extrusion pressures, necessitating a more powerful extrusion motor.

The third major issue is heating the powderbed. The piston used for producing 3-D samples was heated by a band heater from below. This method was successful for experimentation, but probably not sufficient for production of parts. The band heater temperature was controlled to make the powderbed surface reach 100°C, but thermal gradients make this difficult to achieve in thick parts. The temperature in lower layers will approach the flash point of the wax when the upper layers of a thick part reach 100°C. In addition, the time required to heat and cool the powderbed for layering increases as the part

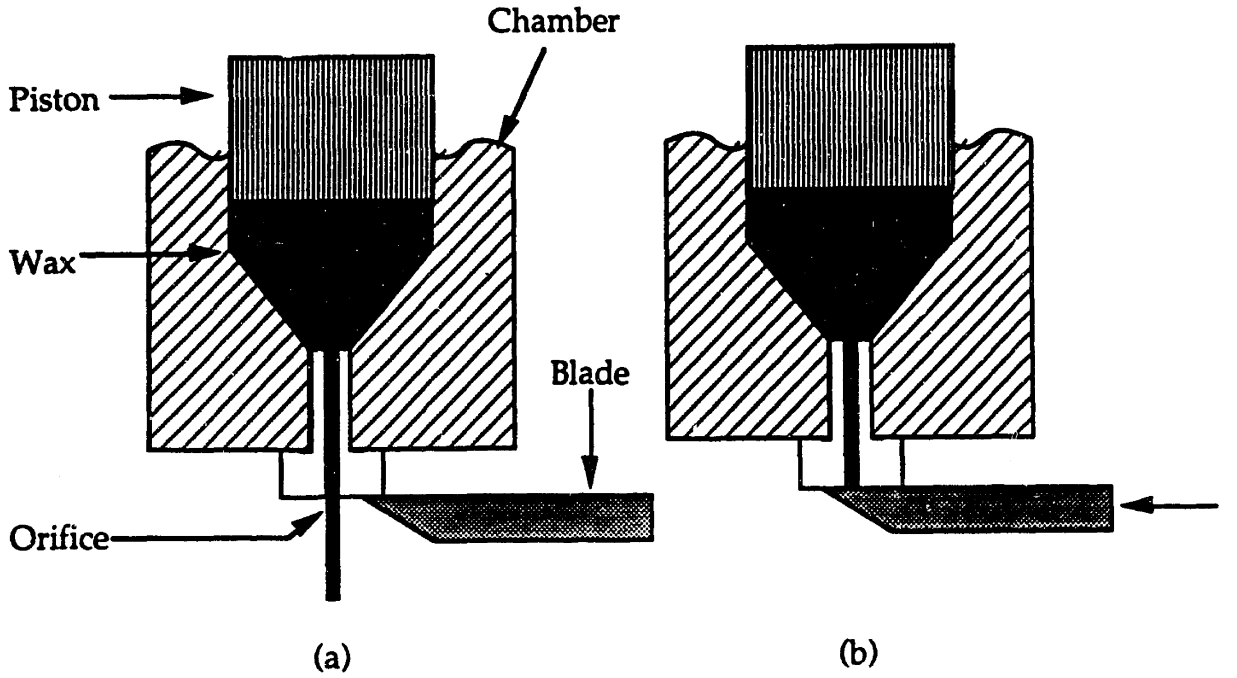

Figure 17. Schematic showing blade method used for severing extruded ligaments. In (a), motor is running; in (b), motor is stopped and blade severs ligament.

becomes thicker. The best solution to this problem is to heat the powderbed convectively from the surface prior to printing a layer. This method allows rapid heat transfer for both heating and cooling.

The fourth major issue is binder placement. This problem will be the final step towards producing loaded wax binder metal parts. It is the final step because all other issues must be resolved before this issue is dealt with. Binder placement will depend on extrusion speed and other process parameters but it will also necessarily depend on factors dealing with binder control that have not yet existed (i.e. how does severing the ligament effect binder delivery?).

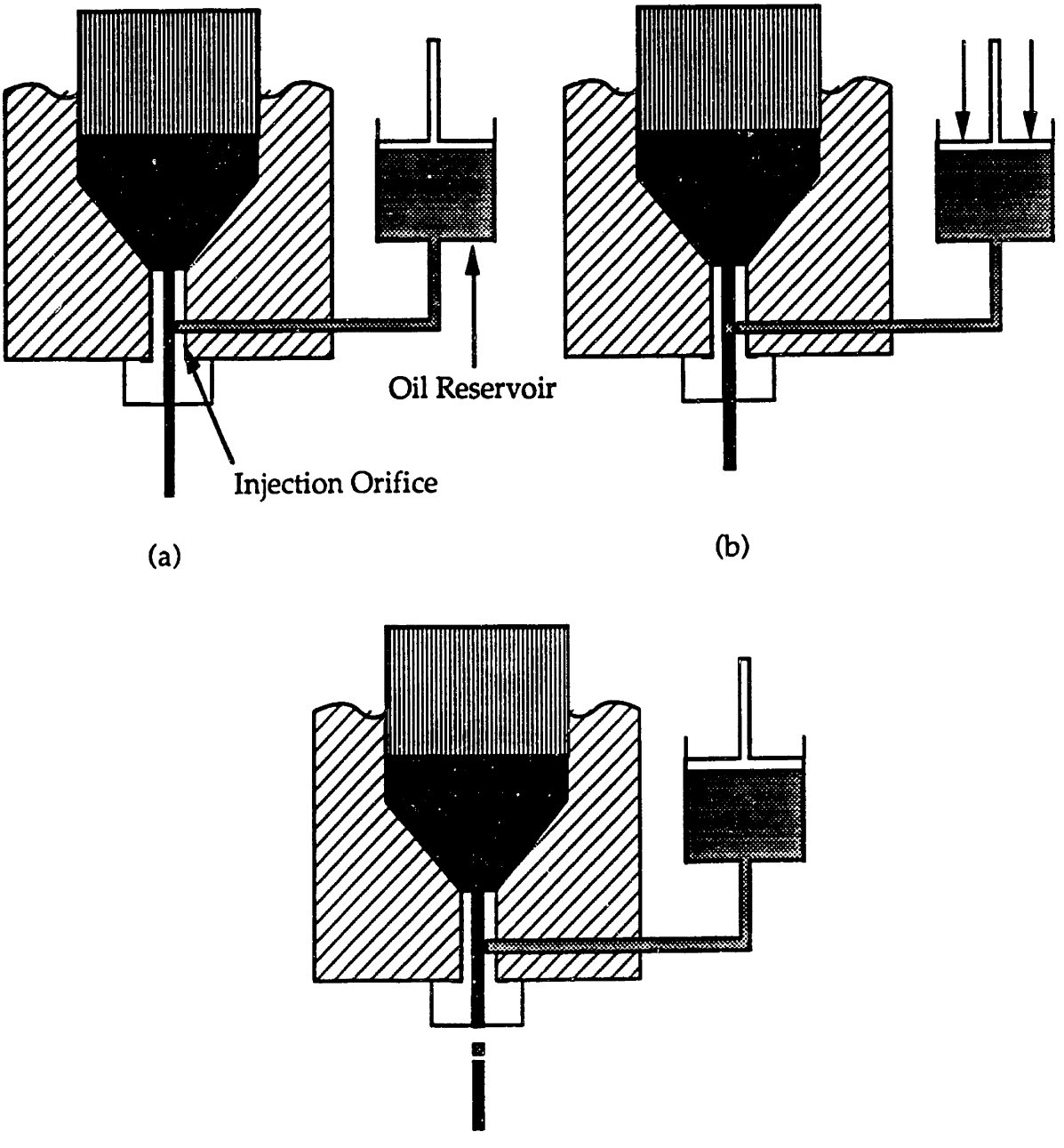

Figure 18. Schematic showing oil injection method used for severing extruded ligaments. In (a), motor is running; in (b), oil is injected into fine extrusion channel; in (c), motor is stopped and ligament separates.

Printing higher volume fraction metal binders is another area which deserves further research. All printing experiments were performed with 33 volume percent metal which produce a final density of approximately 73% when printed on a 60% dense powderbed. Printing higher volume fraction metal binders will further increase green density of printed parts and make the extrusion process more desirable.

References

Adams, R.. Laboratory Notebook, MIT CPRL, Cambridge, 1985.

Bishop, B. A.. *Powder and Polymer Processing of Beta Silicon Carbide, CPRL Report #99.* P. 64, MIT MPC, Cambridge, 1989.

Brady, J. F. and Georges Bossis. *Stoksian Dynamics.* Ann. Rev. Fluid Mech. 1988. 20: Pp. 111-57. Annual Review Inc., 1988.

Dillon, K. R. and R. L. Terchek. *Infiltrated Molded Articles of Spherical, Non-Refractory Metal Powders.* Patent No. 4,431,449, February 14, 1984.

Fowkes, F. M. and R. J. Pugh. *Steric and Electrostatic Contributions to the Colloidal Properties of Non-Aqeous Dispersions.* American Chemical Society, 1984.

German, R. M.. Powder Injection Molding. Pp. 99-120, Metal Powder Industries Federation, Princeton, 1990.

Khanuja, S.. Private communication. October 1992.

Khanuja, S. et al. *Ink Jet Printing of Concentrated Ceramic Suspensions.* To be published, 1994.

Michaels, S. P.. *Production of Metal Parts Using the Three Dimensional Printing Process.* SM Thesis, Pp. 38-45, MIT, 1993.

Shaw, D. J.. Introduction to Colloid and Surface Chemistry. Second Ed., Pp. 16-21, 167-205, Butterworths, London, 1970.